

Synthesis and characterization of PMMA composites activated with starch for immobilization of L-asparaginase

Ahmet Ulu, Suleyman Koytepe, Burhan Ates

Department of Chemistry, Inonu University, Science Faculty, 44280 Malatya, Turkey

Correspondence to: B. Ates (burhan.ates@inonu.edu.tr)

ABSTRACT: Poly (methyl methacrylate) (PMMA)–starch composites were prepared by emulsion polymerization technique for L-asparaginase (L-ASNase) immobilization as highly activated support. The hydroxide groups on the prepared composites offer a very simple, mild and firm combination for enzyme immobilization. The pure PMMA and PMMA-starch composites were characterized as structural, thermal and morphological. PMMA-starch composites were found to have better thermal stability and more hydrophilic character than pure PMMA. L-ASNase was immobilized onto PMMA-starch composites contained the different ratio of starch (1, 3, 5, and 10 wt %). Immobilized L-ASNase showed better performance as compared to the native enzyme in terms of thermal stability and pH. K_m value of immobilized enzyme decreased approximately eightfold compared with the native enzyme. In addition to, immobilized L-ASNase was found to retain 60% of activity after 1-month storage period at 4 °C. Therefore, PMMA-starch composites can be provided more advantageous in terms of enzymatic affinity, thermal, pH and storage stability as L-ASNase immobilization matrix. © 2016 Wiley Periodicals, Inc. *J. Appl. Polym. Sci.* **2016**, *133*, 43421.

KEYWORDS: biodegradable; biomedical applications; biopolymers and renewable polymers; emulsion polymerization

Received 12 October 2015; accepted 7 January 2016

DOI: 10.1002/app.43421

INTRODUCTION

L-asparaginase (EC 3.5.1.1; L-ASNase) is a hydrolytic enzyme that is catalyzed in the conversion of L-asparagine to aspartic acid and ammonia.¹ L-asparagine is a nutritional requirement of both normal and leukemic cells.² The leukemic cells are unable to synthesize the adequate levels of L-asparagine for their metabolism, due to the lack of L-asparagine synthetase, while normal cells can self-synthesize L-asparagine.^{3,4} In the presence of L-ASNase, leukemic cells cannot grow and die because of the lack of protein synthesis.^{5,6} Therefore, this enzyme has been used in certain disease including acute lymphoblastic leukemia (ALL),⁷ lymphosarcoma⁸ and non-Hodgkin's lymphoma,⁹ as a potent anti-tumor or anti-leukemic drug. In spite of its high therapeutic efficacy, prolonged use leads to hypersensitivity, ranging from mild allergic reactions to life-threatening anaphylaxis,¹⁰ due to the high molecular mass of the enzyme and its bacterial origin.¹¹ To reduce the immunological response, prolong the action time and enhance the drug's effects in blood, the native L-ASNase has often been immobilized with various kinds of biocompatible polymers to produce immobilized/modified L-ASNase. The modification or immobilization of the enzyme not only reduced its immunity and toxicity to humans but also greatly improved its resistance to proteolysis in

comparison with native L-ASNase.¹² Several natural or synthetic polymers have been commonly used as the matrix used in the methods of enzyme immobilization. The structure of the matrix material is vitally important to the performance of immobilized enzymes. Nowadays, materials having unique physical properties, wide application potential, more biodegradable and biocompatibility than the polymers have been intensively investigated as the immobilization matrix. In this sense, composites or nanocomposites have attracted the attention of researchers. Therefore, researchers aim to develop novel composite containing natural and high-performance polymers such as starch, chitosan, dextrin etc. for various applications.^{13–17} Examples of such biopolymer that L-ASNase has already been incorporated in are dextran,¹⁸ chitosan,^{19,20} and poly (D,L-lactide-co-glycolide).²¹ Immobilization of enzymes onto composite containing biopolymer allows increased stability to changes in conditions such as pH or temperature. It also may increase resistance to proteases and other denaturing compounds. The use of the starch for enzyme immobilization is preferable to other natural polymers because of the higher reactivity and porosity of starch and/or its lower cost. In our works, the essential aim in the using of starch for the preparation of PMMA composites is the activation of PMMA with

hydroxyl groups of starch for L-ASNase immobilization. PMMA activated with hydroxyl groups can also easily interact with L-ASNase due to the hydrophilic character. Therefore, we investigated PMMA-starch composites as an enzyme immobilization matrix in order to improve L-ASNase half-life and enzymatic stability.

In this study, biodegradable PMMA-starch composites were synthesized by emulsion polymerization using different weight ratios of starch as a biodegradable and biocompatible reinforcement. The obtained composites were characterized by Fourier transform infrared (FT-IR) spectroscopy technique. Thermal analysis techniques such as thermogravimetric analysis (TGA), differential scanning calorimetry (DSC) and differential thermal analysis (DTA) were used for thermal properties of the PMMA-starch composites. The hydrophilicity of the composites was also characterized by water contact angle. The results revealed that the hydrophilicity of the composite samples was significantly and permanently improved. L-ASNase was immobilized onto PMMA-starch composites. Among them, the most appropriate composite (PMMA-S-3%) was selected as the matrix. The surface morphology of the composite was characterized by scanning electron microscopy (SEM) and energy-dispersive X-ray (EDX) analysis. Then, immobilized L-ASNase onto PMMA-starch composite was investigated parameters such as optimum temperature, optimum pH, kinetic parameters and *in vitro* storage stability and compared with native enzyme.

EXPERIMENTAL

Materials and Reagents

L-ASNase, L-asparagine, methyl methacrylate (MMA), sodium dodecyl sulfate (SDS) and Nessler's reagent were purchased from Sigma Ltd. (St. Louis, USA). Starch and tris base were supplied by Merck AG (Darmstadt, Germany). Trichloroacetic acid (TCA) and potassium persulfate ($K_2S_2O_8$) were purchased from Riedel-Haen AG (Darmstadt, Germany). The other chemicals such as solvents, acids and other reagents were analytical grade. Deionized water was used for all preparations.

Characterization

FT-IR spectrum of the samples was recorded in the range of $4000\text{--}400\text{ cm}^{-1}$ using a Mattson 1000 FT-IR spectrometer. The spectra was the result of 30 scans. The spectral resolution was 4 cm^{-1} . The absorption spectra of the samples was recorded as KBr pellets. GPC analysis of pure PMMA was performed at room temperature using THF as eluent at a flow rate of 0.5 mL min^{-1} . A refractive index detector was used as a detector. The instrument (Agilent 1100 series GPC-SEC system) was calibrated with a mixture of polystyrene standards (Polysciences; molecular masses between 200 and 1200,000 Da) using GPC software for the determination of the average molecular masses and polydispersity of the polymer sample. Thermo-gravimetric analysis (TGA) was determined with Shimadzu TGA-50 instrument from room temperature to $800\text{ }^\circ\text{C}$ at a heating rate of $10\text{ }^\circ\text{C min}^{-1}$ under air atmosphere. Differential scanning calorimetry, DSC (Shimadzu DSC-60) was used to measure glass transition temperature (T_g). Differential thermal analysis (DTA) was performed using Shimadzu DTA-50 in temperature range room temperature to $800\text{ }^\circ\text{C}$ at a heating rate $10\text{ }^\circ\text{C per minute}$.

The surface morphology, porosity and fractured surface of the samples were observed by scanning electron microscope (SEM). The SEM images were acquired on LEO Evo-40 VPX scanning electron microscope in the secondary electron imaging mode. Emission current was $10\text{ }\mu\text{A}$, accelerating voltage was 2 kV , and the working distance was 3 mm for the analysis. Carbon tape (Spectro tabs, 12 mm O.D.) attached to the aluminum specimen stubs were used for the sample preparation; pressured air was applied to remove the loosely attached particles. Samples for SEM analysis were sputter coated with Au/Pd using a sputter coater (Bal-Tec SCB 050). Chemical composition analysis by EDX was performed with an EDX; Rönbeck Xflash detector analyzer associated to a scanning electron microscope (SEM, Leo-Evo 40xVP). The incident electron beam energy was varied from 3 to 30 keV . In all cases, the beam was at normal incidence to the sample surface and the measurement time was 100 s .

The water contact angles were measured using an SEO Phoenix 300 contact angle measuring apparatus. A Shimadzu UV-vis spectrophotometer (UV-vis 1601, Shimadzu) was used to analyze the activity of the both native and immobilized enzymes at 480 nm .

Preparation of PMMA

The PMMA was synthesized by emulsion polymerization method of methyl methacrylate monomer. Methyl methacrylate (MMA, 10 mL) and surfactant sodium dodecyl sulfate (SDS, 0.04 g) were added into 100-mL Schlenk flask and stirred for 30 min with a nitrogen line and a magnetic stirrer. An aqueous solution of potassium persulfate (KPS, 0.5 g) was subsequently added to the medium. Then, the mixture was heated in a water bath with a magnetic stirrer heating until $80\text{ }^\circ\text{C}$. The polymerization was maintained for $3\text{--}4\text{ h}$ at $80\text{--}90\text{ }^\circ\text{C}$. The polymer was filtered, washed with water to demulsify, dried at $50\text{ }^\circ\text{C}$. After that, the poly (methyl methacrylate) particles were pulverized and were named as PMMA (yield was about 90%).

Preparation of PMMA-Starch Composites

PMMA-starch composites were performed in a 100-mL Schlenk flask equipped with a nitrogen line and a condenser. For the synthesis of PMMA-starch composites, the monomer MMA and various weight percentage of starch ($1, 3, 5,$ and $10\text{ wt } \%$) were dispersed in 100 mL of water containing 0.04 g of SDS and stirred for 30 min with a magnetic stirrer. An aqueous solution of potassium persulfate (0.5 g) was subsequently added to the medium. Then, the mixture was heated in a water bath with a magnetic stirrer heating until $80\text{ }^\circ\text{C}$ and the polymerization was maintained for $3\text{--}4\text{ h}$ at $80\text{--}90\text{ }^\circ\text{C}$. Thereafter the Schlenk flask was removed from the water bath and it was cooled to room temperature. The prepared PMMA-starch composites were collected by filtration and washed several times with distilled warm water to remove unreacted starch from the composites. The samples were dried in a vacuum oven at $50\text{ }^\circ\text{C}$ for 24 h and were pulverized. After, the samples were named as PMMA-S-1%, PMMA-S-3%, PMMA-S-5%, and PMMA-S-10%, respectively.

Preparation of L-Asparaginase Immobilized PMMA-Starch Composites

Nearly 0.1 g of pure PMMA and PMMA-starch composite samples were added to Eppendorf tubes containing distilled water (0.75 mL) and L-ASNase (100 IU) and were stirred for 30 min

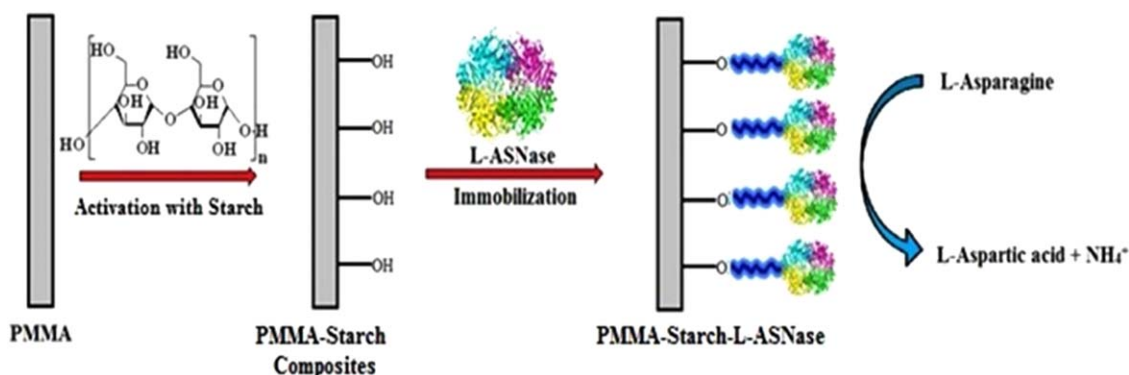


Figure 1. Schematic image of preparation and effect mechanism of PMMA-starch-L-ASNase. [Color figure can be viewed in the online issue, which is available at wileyonlinelibrary.com.]

with an orbital shaker at 4 °C, respectively. Then, the mixture was centrifuged at 5000 rpm for 5 min at 4 °C. Following of centrifugation, the supernatants were taken and unbound enzyme was removed by washing the solid with sterilized distilled water. Finally, the solid containing L-ASNase was dried using a vacuum evaporator. Schematic image of preparation and effect mechanism of PMMA-Starch-L-ASNase composites was illustrated in Figure 1. The solid sample (5 mg) was taken to measure the enzyme activity. PMMA-starch composites have free volume for L-ASNase immobilization. It was determined that PMMA-S-3% has optimum free volume for L-ASNase compared with other synthesized materials. The free volumes of PMMA-S-5% and PMMA-S-10% are higher than other PMMA-starch composites. In these composites, activities of immobilized L-ASNase decreased in compared with PMMA-S-3%-LASNase. These declines are due to leaching of the enzyme from the free volume of PMMA-S-5% and PMMA-S-10%. Therefore, PMMA-S-3% was used as the model matrix for determination of immobilization parameters due to the highest activity of PMMA-S-3%-L-ASNase (Table I).

Biodegradation Study of Pure PMMA and PMMA–Starch Composites

The samples of pure PMMA and PMMA-starch composites were weighed 0.1 g and were placed in biodegradation medium. The medium composition was prepared as 50 mM phosphate buffer solution (PBS) of pH 7.4. Each sample (0.1 g) was placed into an individual vial containing 10 mL PBS, and incubated at 37 °C. The samples were taken out after 1, 2, and 4 weeks and washed with distilled water. The samples were dried in a vacuum oven at room temperature for 2 days and were reweighed to determine the weight loss percent using the following formula:

$$\text{Weight loss (\%)} = \left(m_o - \frac{m_d}{m_o} \right) \times 100$$

where m_o and m_d are the masses of pure polymer and composites before and after biodegradation. All experiments were performed in triplicate.

Activity Assays of Native and Immobilized L-Asparaginase

The native and immobilized L-ASNase activity were measured based on the amount of released ammonia during the hydrolysis of the substrate using Nessler's reagent, as described by Mashburn and Wriston.²¹ The reaction mixture contained 1 mL of 10 mM L-asparagine (prepared with 0.05M Tris-HCl pH: 8.6) and the sample (native LASNase: 5 IU, PMMA-S-LASNase: 5 mg). The mixture was incubated for 30 min at 37 °C, after the reaction was terminated by the addition of 0.01 mL of 1.5M trichloroacetic acid (TCA) and then, centrifuged to separate the precipitated protein from the solution. The liberated ammonia was determined by adding 0.25 mL of Nessler's reagent. All experiments were performed in triplicate. The absorbance was recorded at 480 nm after 10 min. L-asparaginase activity was defined as mmol of NH₄⁺ formed per minute and expressed in IU.²²

Effect of pH and Temperature on the Enzymatic Activity of Native and Immobilized L-Asparaginase

The effect of pH on the enzyme activity on both native and immobilized L-ASNase was examined using acetate buffer (pH; 4.0, 5.0, 6.0) and Tris-HCl buffer (pH; 7.0, 7.5, 8.0, 8.5, 9.0, 10.0) at 37 °C. The optimal temperature of the native and immobilized L-ASNase was determined by measuring in the temperature range of 25–65 °C in Tris-HCl (50 mM, pH 8.6). All these reactions were performed according to the method in the activity assays of native and immobilized L-asparaginase. All experiments were performed in triplicate. The highest activity was expressed as 100% and all activity values were given in comparison to 100% as relative activity.

Kinetic Analysis of Native and Immobilized L-Asparaginase

To obtain the kinetic parameters of native and immobilized L-ASNase were measured the enzymatic activity in 50 mM Tris-HCl (pH 8.6) at 37 °C with different concentrations (0.1, 0.5, 1.0, 2.0, 5.0, 10.0, 20.0, and 50.0 mM) of L-asparagine as substrate. All experiments were performed in triplicate. The kinetic parameters (V_{\max} and K_m) of L-ASNase under the native and immobilized

Table I. Relative Enzyme Activities and the Contact Angles of Pure PMMA and PMMA–Starch Composites

Sample	Relative activity (%)	Contact angle (°)
PMMA	0.9	85.44
PMMA-S-1%	68.9	72.92
PMMA-S-3%	100	62.92
PMMA-S-5%	56.4	50.95
PMMA-S-10%	47.5	35.18

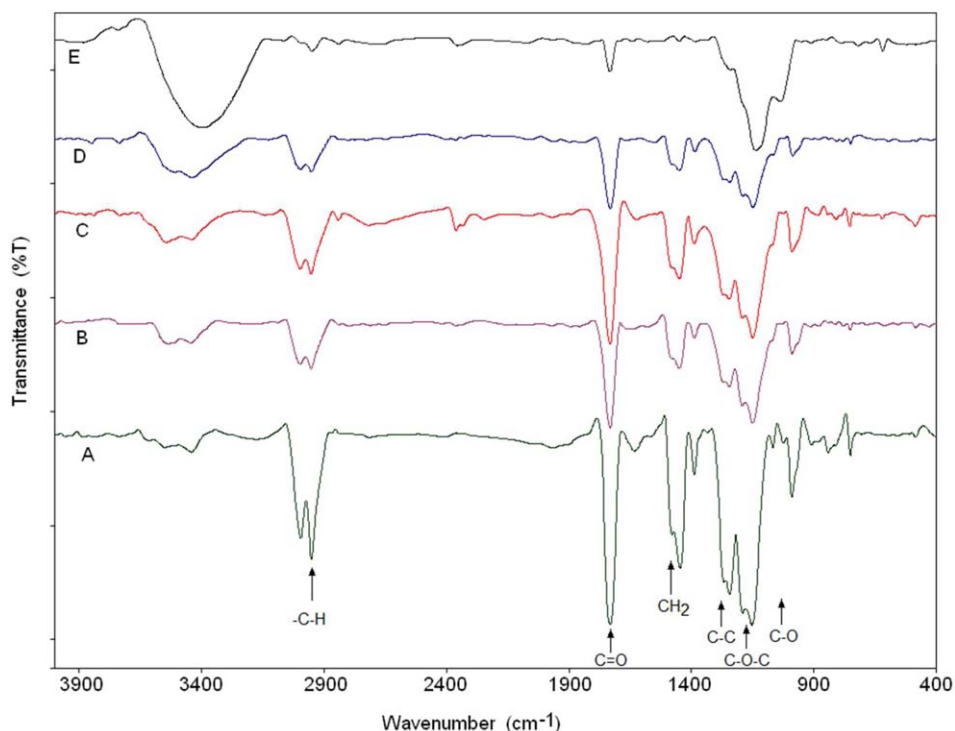


Figure 2. FT-IR spectra of (A) PMMA, (B) PMMA-S-1%, (C) PMMA-S-3%, (D) PMMA-S-5%, (E) PMMA-S-10%. [Color figure can be viewed in the online issue, which is available at wileyonlinelibrary.com.]

conditions were calculated from a Lineweaver–Burk equation. Protein concentration was estimated with Bradford method using bovine serum albumin as a standard.²³

Storage Stability of Native and Immobilized L-Asparaginase

The storage stability of native and immobilized L-ASNase at 4 and 25 °C was measured by calculating the residual activity for a month. All experiments were performed in triplicate. Samples were taken at different time intervals during incubation, and the relative activity was determined using the method described in the enzyme assay.

RESULTS AND DISCUSSION

FT-IR Analysis of Pure PMMA and PMMA–Starch Composites

The pure PMMA and PMMA-starch composites were developed from *in situ* emulsion polymerization of methyl methacrylate and different ratio starch in the presence of sodium dodecyl sulfate. The FT-IR bands of the pure PMMA and PMMA–starch composite were shown in Figure 2. In this figure, the sharp peak correspond to the carboxyl group of the acrylate of pure PMMA was at 1735 cm^{-1} .²⁴ A intense peak appeared ranging from 2899 to 2950 cm^{-1} due to the presence of aliphatic CH_2 stretching vibration. The peaks at 1274 cm^{-1} were assigned to C–O stretching vibration of the ester bond. Other peaks at 1195 cm^{-1} , 1144 cm^{-1} were assigned to $-\text{O}-\text{CH}_3$ stretching vibrations and CH_3 stretching, respectively. It was clear that all of the composites was the same peak. However, sharp of the $-\text{O}-\text{CH}_3$ and C=O peaks reduced with the addition of the starch into PMMA. This reduction could be due to the hydrogen bonding between the O–H group of starch and the acrylic

group of PMMA.²⁵ From the Figure 2, a strong and broad peak at 3200–3600 cm^{-1} was assigned to the characteristic absorption peak due to the stretching vibrations of O–H. In conclusion, we successfully synthesized a series of PMMA–starch composites.

GPC Analysis of Pure PMMA

The weight-average molecular weight (M_w), number-average molecular weight (M_n) and polydispersity (PDI: M_w/M_n) of pure PMMA were obtained by GPC analysis. M_w and M_n values of PMMA were determined as 258,070 and 197,000 g mol^{-1} , respectively. Also, the PDI value of the PMMA was calculated as 1.31. On the basis of these results, we can deduce that pure PMMA with a unimodal molecular weight distribution and a low polydispersity index was obtained.

Thermal Analysis of Pure PMMA and PMMA–Starch Composites

The TGA curves of pure PMMA and PMMA-starch composites in the temperature range from 20 °C to 800 °C were compared in Figure 3. The TGA curve presented that pure PMMA decomposed in two stages. The first stage assigned roughly 5% weight loss ratio at between 200 and 350 °C. This mass loss indicated that degradation of the side groups in the polymeric structure. The second loss peak (~90%) starting at above 350 °C was ascribed to thermal degradation of the PMMA.²⁶ In the thermogram of PMMA-starch composite, initial decomposition temperature was shifted lower temperatures.

Figure 4 shows DTA curves of pure PMMA and PMMA–starch composite. In this thermogram, in the temperature range of thermal decomposition of pure PMMA a sharp endotherm peak. DTA results were also parallel with TGA thermograms.

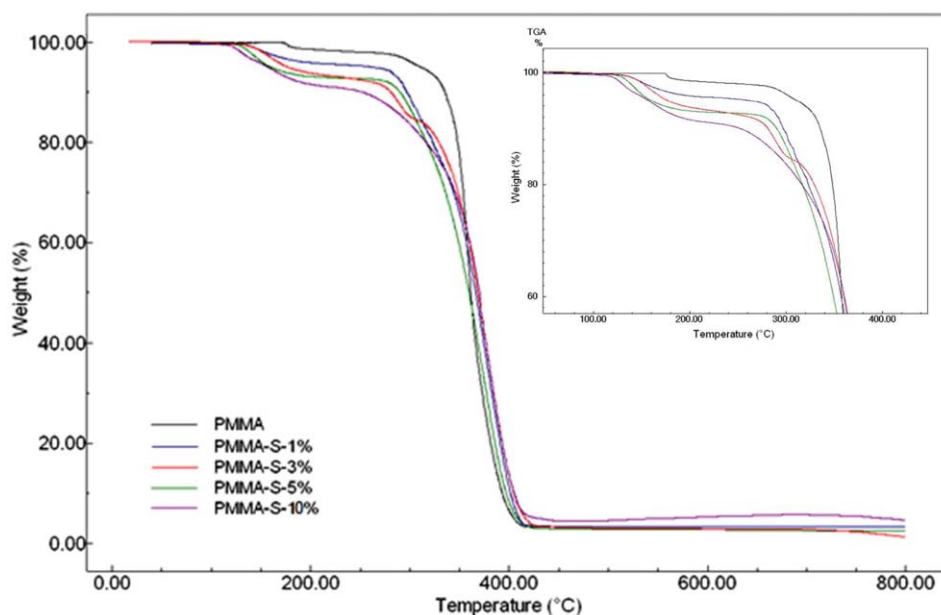


Figure 3. TGA thermograms of pure PMMA and PMMA–starch composites. [Color figure can be viewed in the online issue, which is available at wileyonlinelibrary.com.]

DSC curves of pure PMMA and PMMA–starch composites containing different proportions starch were given in Figure 5. From these curves, glass transition temperature (T_g) for the pure PMMA was determined at 110 °C. This T_g value is very similar in literature.²⁷ As can be seen in Figure 5, T_g values of PMMA-S-1%, PMMA-S-3%, PMMA-S-5%, and PMMA-S-10% were determined as 119, 122, 130, and 147 °C, respectively. The increase of T_g values caused high interaction between chains and obtained rigid structure depending on the amount of starch.²⁸

Presence of Enzyme Binding

The binding of L-ASNase to PMMA-starch composite was approved by FT-IR analysis. The FT-IR spectra in Figure 6 represent the spectra of PMMA, PMMA-S-3% and of PMMA-S-3%-L-ASNase. As we look at the spectra in detail, PMMA-S-3%-L-ASNase also displays all of characteristic bands.²⁹ However; a decrease in the band intensity of the stretching can be seen in this spectrum. Thus, it can be indicated that the enzyme was successfully immobilized the composite support material.

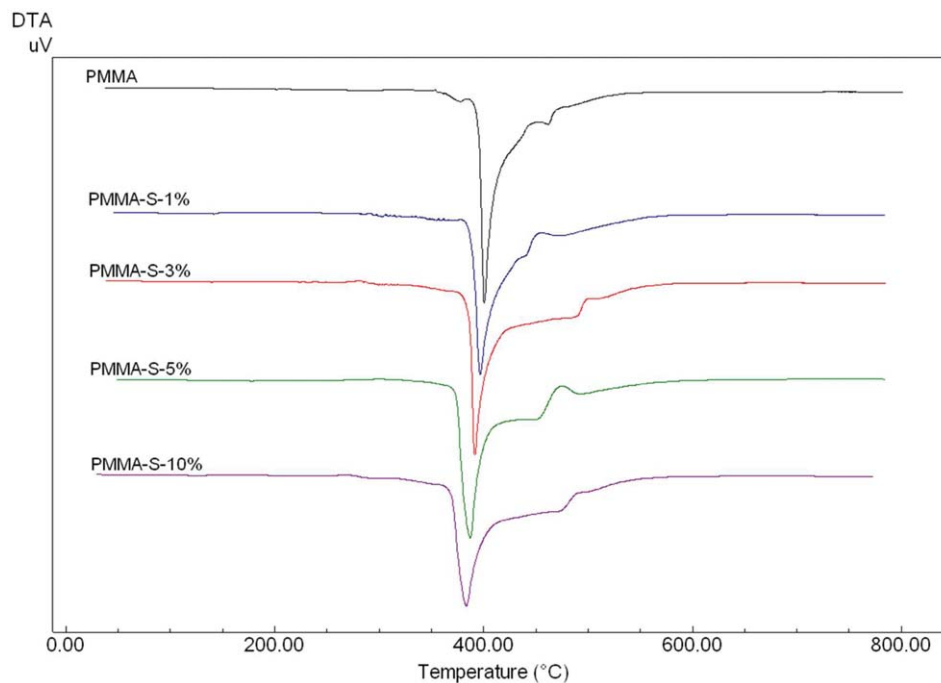


Figure 4. DTA thermograms of pure PMMA and PMMA–starch composites. [Color figure can be viewed in the online issue, which is available at wileyonlinelibrary.com.]

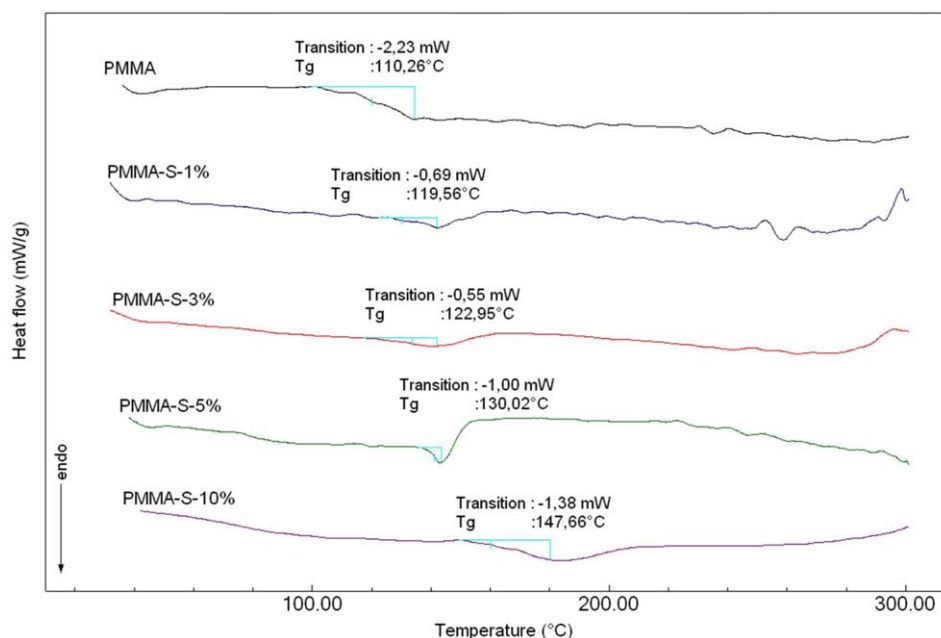


Figure 5. DSC thermograms of pure PMMA and PMMA–starch composites. [Color figure can be viewed in the online issue, which is available at wileyonlinelibrary.com.]

To investigate the influence of L-ASNase incorporated into the PMMA/starch composites on the morphology, PMMA and PMMA-S-3%-L-ASNase were examined by scanning electron microscopy. Figure 7 represents the typical SEM images of PMMA and PMMA-S-3%-L-ASNase with high and low magnification. It has been reported that the morphology of PMMA-S-3%-L-ASNase is found to be very fragmental in shape.

EDX spectra of the PMMA and PMMA-S-3%-L-ASNase were collected and investigated to determine the presence of enzyme in the polymeric matrix (Figure 8). The presence of N and S can be clearly seen from the EDX spectra of PMMA-S-3%-L-ASNase. Thus, the EDX analysis confirmed that L-ASNase was successfully incorporated into PMMA-starch composites structure.

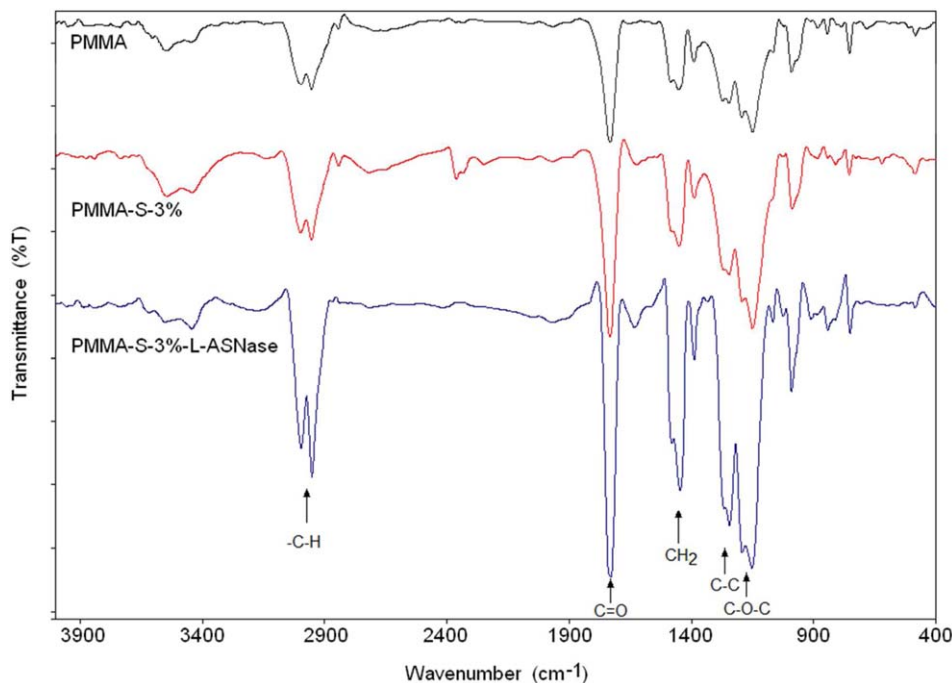


Figure 6. FT-IR spectra of the pure PMMA, PMMA-S-3% and PMMA-S-3%-L-ASNase. [Color figure can be viewed in the online issue, which is available at wileyonlinelibrary.com.]

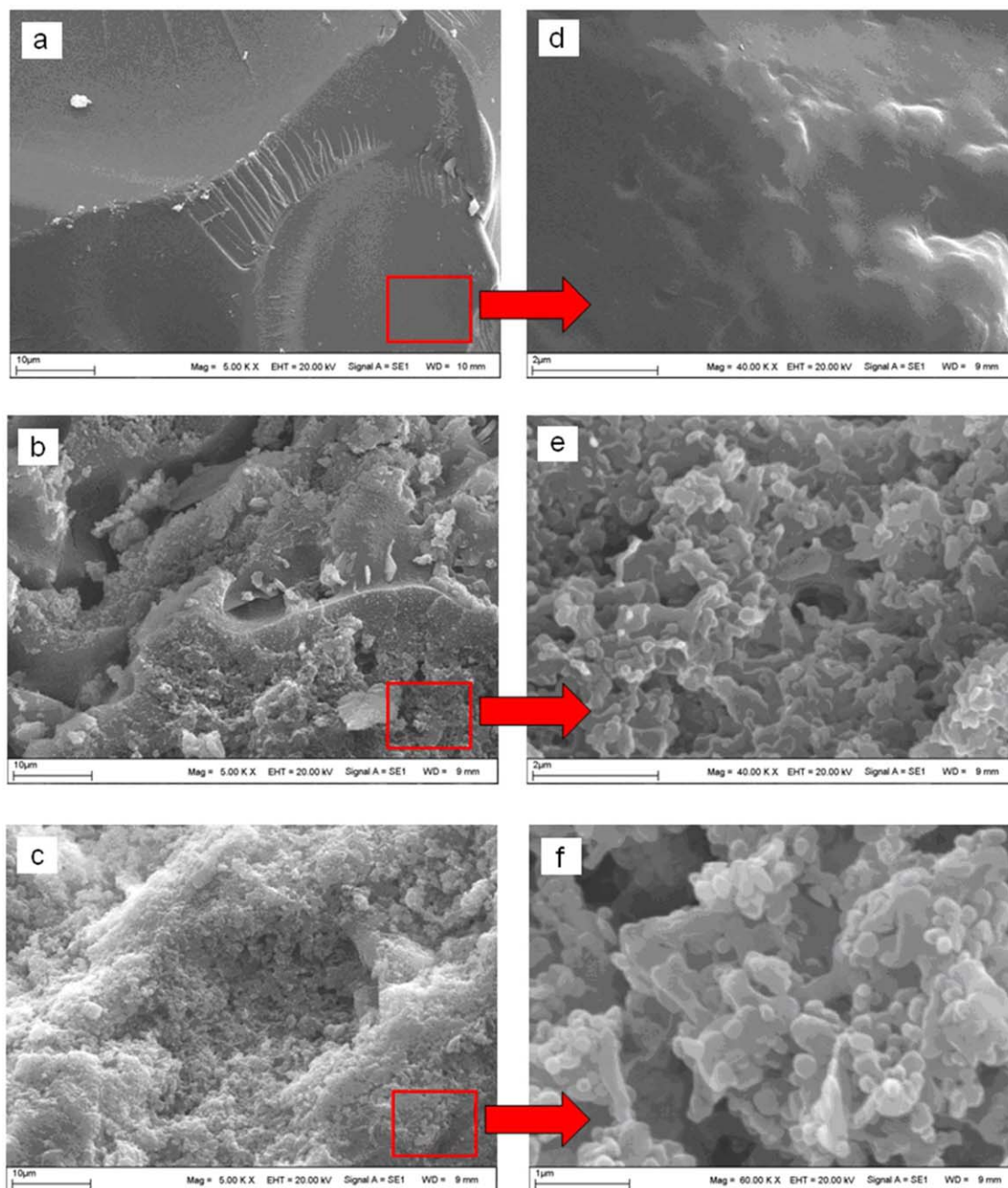


Figure 7. SEM image of the pure PMMA (a,d), PMMA-S-3% (b,e) and PMMA-S-3%-L-ASNase (c,f). (a, b and c are low magnification. d, e and f are high magnification). [Color figure can be viewed in the online issue, which is available at wileyonlinelibrary.com.]

Measurements of Contact Angle

We measured contact angle of samples using a Wilhelmy plate technique and calculated average of three measurements. Table I shows the contact angles of pure PMMA and PMMA-starch composites. The contact angle of PMMA surfaces was 85.44° . In the literature, for PMMA, the contact angle values ranged from 79° to 117° .³⁰ The measured value is consistent with the literature. The wettability of composite films increased with the amount of starch. The contact angles of PMMA-S-1%, PMMA-S-3%, PMMA-S-5%, and PMMA-S-10% films were measured as 72.92° , 62.92° , 50.95° , and 35.18° , respectively.

Biodegradation Study

PMMA has low biodegradability as enzyme immobilization matrix. Thus, the biodegradability of PMMA can also be enhanced by incorporating of the natural and easily degradable molecules into the polymer structure. Starch as easily degradable molecule is one of the promising materials for the production of biodegradable plastics. Starch has been incorporated into polyethylene in order to increase the biodegradability. In this study, to increase the biodegradability of the PMMA, different ratios of starch was used. The biodegradation of PMMA-starch composites was compared with pure PMMA in a study for 1 month during 7th, 14th, and 28th

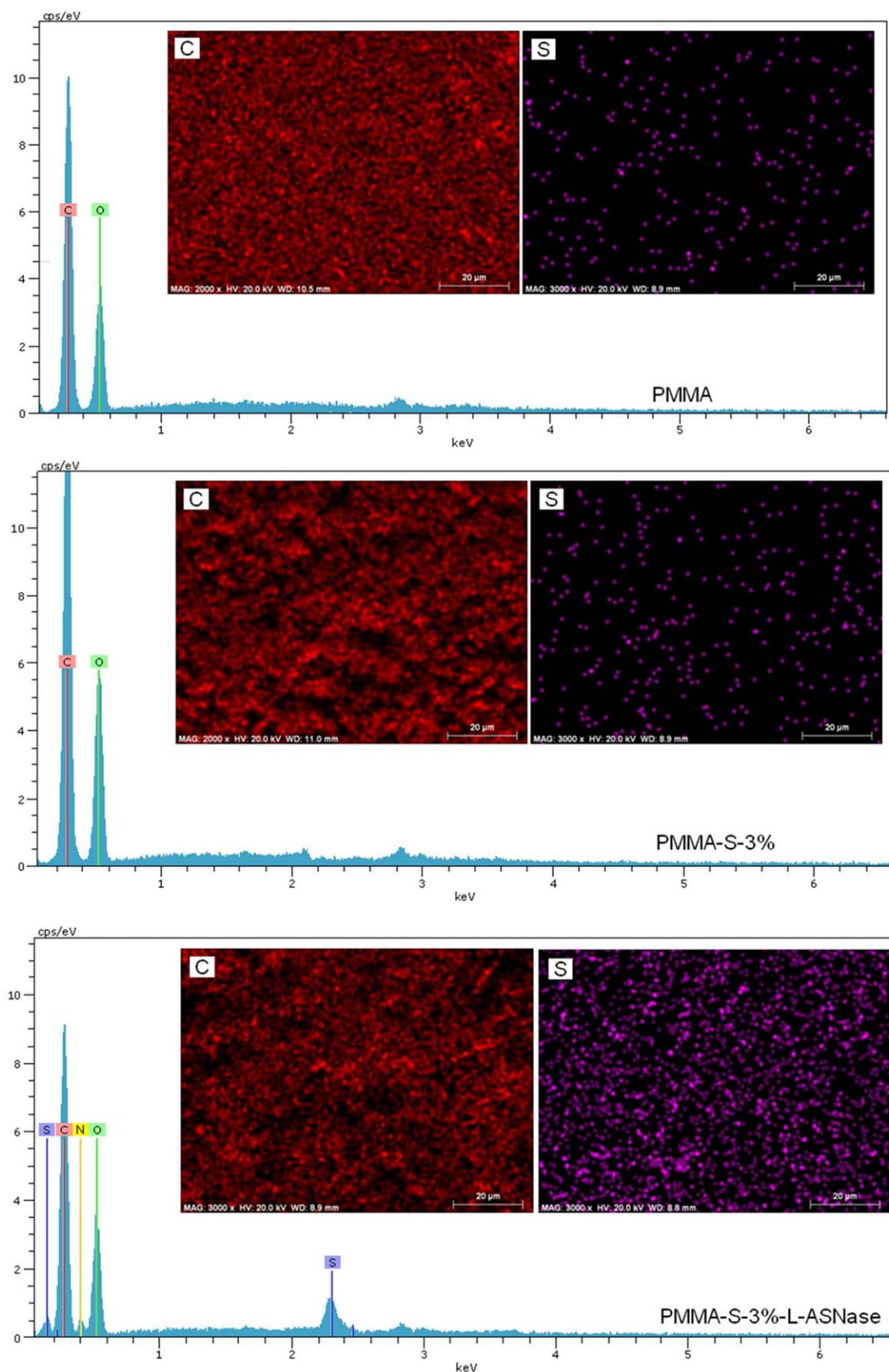


Figure 8. EDX spectra and EDX-mapping of the pure PMMA and PMMA-S-3%-L-ASNase. [Color figure can be viewed in the online issue, which is available at wileyonlinelibrary.com.]

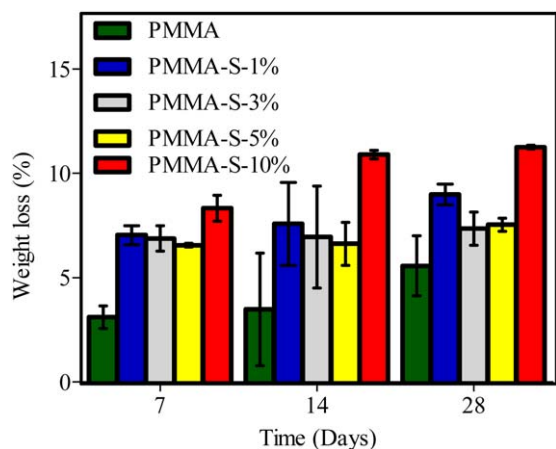


Figure 9. The biodegradation of pure PMMA and PMMA-starch composites. Each value is the average of triplicate experiments with error bars indicating STDEVs(σ_{n-1}). [Color figure can be viewed in the online issue, which is available at wileyonlinelibrary.com.]

days. Degradation results were shown by calculating percentage weight loss in Figure 9. It was found that the percentage of weight loss in composites were increased with the ratio of starch compared with pure PMMA. Biodegradability of the composite is related to the amount of starch and interactions between PMMA and starch. PMMA-S-3% and PMMA-S-5% have same or low biodegradability compared with PMMA-S-1%. It can be explained with strong interactions between the PMMA and starch. It is formed more compact with stacked polymer chain structure. The good interaction between starch and the polymer affects chemical and thermal stability and biodegradability of this stacked structure decreases. Another effect in biodegradability properties of the composites is the most hydrophilic character in high starch concentration. Especially, in PMMA-S-10%, the incorporating of the starch caused the high increase in the hydrophilic character of PMMA-starch. Therefore, this composite has more hydrolytic biodegradability compared with other PMMA-starch composites.

Effect of pH and Temperature on the Enzymatic Activity of Native and PMMA-S-3%-L-ASNase

The effect of pH on the activities of native L-ASNase and PMMA-S-3%-L-ASNase was studied by changing the pH of different buffer from 4.0 to 10.0. The results were shown in Figure 10(a). The both native and immobilized L-ASNase showed an optimal pH as 8.5. This result was consistent with previous studies based on chemical modification of L-ASNase by immobilization with chitosan-tripolyphosphate nanoparticles¹⁹ and calcium alginate-gelatine composites.³¹ However, immobilized L-ASNase exhibited at high activity above 60% in the between pH values of 7.0 and 10.0 and immobilized enzyme showed more catalytic activity and stability under alkaline media. It is explained that PMMA is less affected with pH due to the inert character of PMMA. When the obtained results compared with different techniques in the literature, in a study of Ashrafi *et al.*, L-ASNase was covalently immobilized onto fatty acids having different chain lengths. Increasing of activity of the immobilized L-ASNase was only determined approximately 20% under in the range from pH 7.0 to 10.0.³² In the study of Zhang *et al.*, they synthesized silk sericin peptides–

L-ASNase bioconjugates via covalent modification. Residual activity of silk sericin peptides–L-ASNase was ~ 20 –40% the pH of from 7.0 to 10.0, even the native enzyme was more stable than the immobilized enzyme.¹² According to these works, we can report that our results are more advantageous in term of pH resistance.

Thermal stability experiments were carried out for native and PMMA-S-3%-L-ASNase, incubated at different temperatures ranging from 25 to 60 °C. The experimental data obtained for both native and immobilized enzymes were shown in Figure 10(b). The optimal temperature was 45 °C for the native and immobilized enzyme. The results showed that high temperatures (55 and 60 °C) caused to total inactivation of the native enzyme. This expressive inactivation is attributed to a higher vibration of the atoms of the protein caused by high temperatures, which may break some chemical bonds resulting in drastic changes of its 3D structure.³³ Although residual activity of native enzyme was 30% at 55 °C, residual activity of

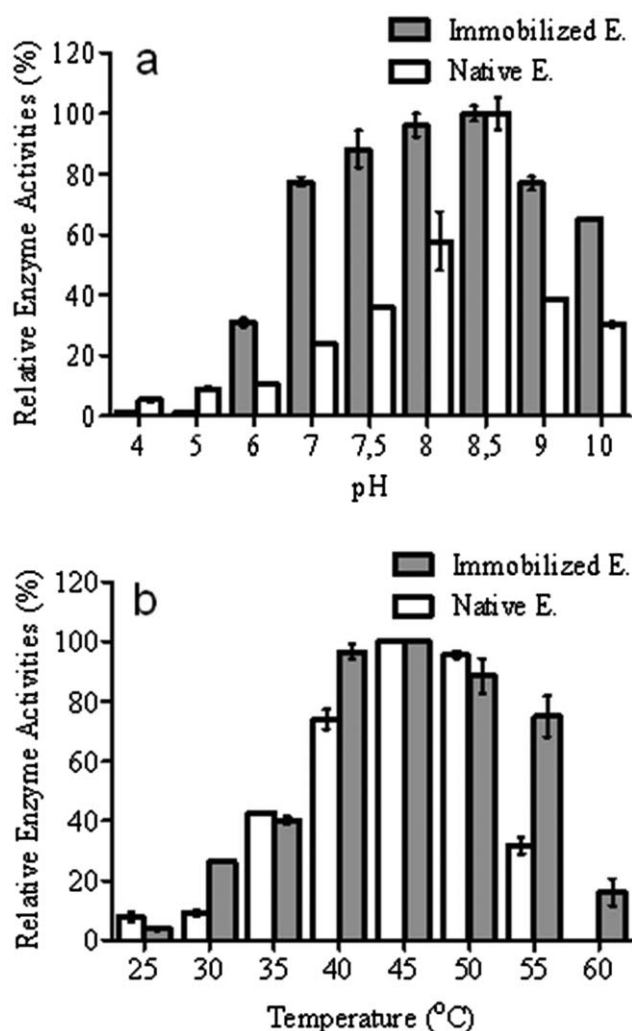


Figure 10. (a) Effect of pH on activities of native and immobilized L-asparaginase. Each value is the average of triplicate experiments with error bars indicating STDEVs(σ_{n-1}). (b) Effect of temperature on activities of native and immobilized L-asparaginase. Each value is the average of triplicate experiments with error bars indicating STDEVs(σ_{n-1}).

Table II. Kinetic Parameters of Native and Immobilized Enzyme

Enzyme	Substrate	K_m (mM)	V_{Max} (U mg ⁻¹ protein)
Native enzyme	L-asparagine	0.216	301
Immobilized enzyme	L-asparagine	0.0256	253

immobilized enzyme was 80%. In addition, while the native enzyme denatured at above of 55 °C, even the immobilized enzyme was able to maintain rate to ~20% of its activity at 60 °C. That is why protected the active center and structure of the enzyme after immobilization. Vina *et al.* reported that immobilization of L-ASNase on polysaccharide levan. Their studies evidenced that the residual activity of immobilized enzyme was measured as ~70% at 50 °C.²² Zhang *et al.* prepared silk fibroin nanoparticle-L-ASNase bioconjugates and determined optimal conditions of the enzyme.³⁴ According to effects of reaction temperature on immobilized L-ASNase, optimal temperature was 50 °C for the native and the immobilized enzyme. However, the native enzyme was more thermally stable than the immobilized enzyme at 60 °C.

In conclusion, we determined high enzymatic activity in large pH and temperature scale for immobilized L-ASNase than compared with literature. These advantages of the immobilized L-ASNase make it a good candidate in the different applications.

Kinetic Analysis of Native and PMMA-S-3%-L-ASNase

Reaction kinetics were analyzed for native and PMMA-S-3%-L-ASNase in Tris-HCl buffer, pH 8.6, at 37 °C using different concentrations of L-asparagine. The classical Lineweaver-Burk model was used to determine these kinetic parameters. The kinetic parameters of the native and immobilized L-ASNase were listed in Table II. The obtained K_m and V_{max} values were of 0.216 mM and 301 U mg⁻¹ protein for native enzyme and 0.0256 mM and 253 U mg⁻¹ protein for immobilized L-ASNase, respectively. These results show that native and immobilized L-ASNase present distinct behaviors. For comparison, it could be observed that the K_m value of PMMA-S-3%-L-ASNase was approximately eight lower than native enzyme. It is shown

that the affinity between L-ASNase and its substrate asparagine was considerably increased when L-ASNase was immobilized on the PMMA-starch composite. V_{max} decreases about 1.2 times for immobilized L-ASNase when compared to native L-ASNase. This decrease in V_{max} is in agreement with the results reported in literature comparing native and immobilized enzymes.³⁵

Storage Stability of Native and PMMA-S-3%-L-ASNase

The native and PMMA-S-3%-L-ASNase were incubated at 4 °C and room temperature to measure the residual activity for 30 days. The results were shown in Figure 11. In general, there were no notable differences between the residual activities of both native and immobilize L-ASNase after incubated at 4 °C. However, the end for 15 days at 25 °C, even though the native enzyme progressively lost initial activity, the immobilized enzyme showed 20% initial activity. This evident that the modification of enzyme with PMMA-starch considerably enhanced the resistance to room temperature.

CONCLUSIONS

In the present work, L-ASNase was successfully immobilized onto biodegradable and biocompatible PMMA-starch composites. The hydroxyl groups of starch provide interaction between L-ASNase and PMMA-starch composites. Therefore, while PMMA-starch-L-ASNase showed high activity, PMMA-L-ASNase exhibited little or no activity. The affinity of the immobilized L-ASNase increased considerably compared with that of native enzyme in terms of the thermal, pH and storage stabilities. The immobilization process advanced the L-ASNase thermal stability above 60 °C and pH activity range from pH 8.5 to pH 10.0. The K_m values were 0.216 and 0.026 mM for native and immobilized enzyme, respectively. The affinity of L-ASNase with its substrate L-asparagine increased considerably when modified with the PMMA-S-3%. As a result of, PMMA-starch composite prepared by *in situ* doping of starch to PMMA can be provided more advantageous in term of enzymatic affinity, thermal, pH and storage stability for L-ASNase immobilization.

ACKNOWLEDGMENTS

This work was partially supported by The Inonu University Scientific Research Projects Unit (Grant No. BAP 2013/37).

REFERENCES

- Ramya, L. N.; Doble, M.; Rekha, V. P. B.; Pulicherla, K. K. *Appl. Biochem. Biotechnol.* **2012**, *167*, 2144.
- McCredie, K. B.; Ho, D. H. W.; Freireich, E. J. *CACancer J. Clin.* **2008**, *23*, 220.
- Zhang, Y. Q.; Zhou, W. L.; Shen, W. D.; Chen, Y. H.; Zha, X. M.; Shirai, K.; Kiguchi, K. *J. Biotechnol.* **2005**, *120*, 315.
- Haley, E. E.; Fischer, G. A.; Welch, A. D. *Cancer Res.* **1961**, *21*, 532.
- Jain, R.; Zaidi, K. U.; Verma, Y.; Saxena, P. *People's J. Sci. Res.* **2012**, *5*, 29.
- Savitri, S.; Asthana, N.; Azmi, W. *Indian J. Biotechnol.* **2003**, *2*, 184.

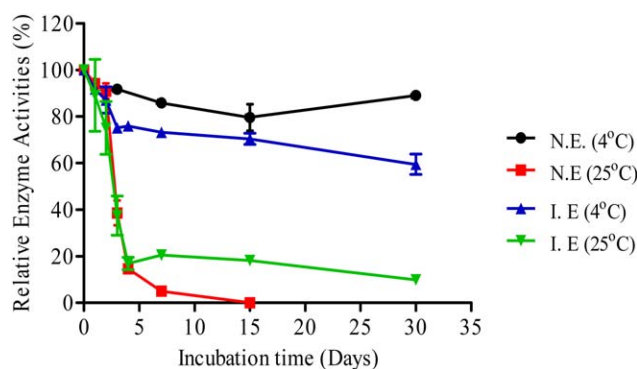


Figure 11. The storage stabilities of immobilized enzyme incubated at 4 and 25 °C. Each value is the average of triplicate experiments with error bars indicating STDEVs (σ_{n-1}). [Color figure can be viewed in the online issue, which is available at wileyonlinelibrary.com.]

7. Hill, J. M.; Roberts, J.; Loeb, E.; Khan, A.; MacLellan, A.; Hill, R. W. *J. Am. Med. Assoc.* **1967**, *202*, 882.
8. Beard, M. E.; Crowther, D.; Galton, D. A.; Guyer, R. J.; Fairley, G. H.; Kay, H. E.; Knapton, P. J.; Malpas, J. S.; Scott, R. B. *Br. Med. J.* **1970**, *1*, 191.
9. Kobrinsky, N. L.; Sposto, R.; Shah, N. R.; Anderson, J. R.; DeLaat, C.; Morse, M.; Warkentin, P.; Gilchrist, G. S.; Cohen, M. D.; Shina, D. *J. Clin. Oncol.* **2001**, *19*, 2390.
10. Shrivastava, A.; Khan, A. A.; Khurshid, M.; Kalamb, M. A.; Jain, S. K.; Singhal, P. K. *Crit. Rev. Oncol. Hematol.* **2015** (in press).
11. Ruysen, R.; Lawers, A. Asparaginase, in *Pharmaceutical Enzymes: Properties and Assay Methods*; Story-Scientia: Gent, **1978**, p 191.
12. Zhang, Y. Q.; Tao, M. L.; Shen, W. D.; Mao, J. P.; Chen, Y. H. *J. Chem. Technol. Biotechnol.* **2006**, *81*, 136.
13. Lakouraj, M. M.; Mojerlou, F.; Zare, E. N. *Carbohydr. Polym.* **2014**, *106*, 34.
14. Rhim, J. W.; Hong, S. I.; Park, H. M.; Ng, P. K. W. *J. Agric. Food Chem.* **2006**, *54*, 5814.
15. Zare, E. N.; Lakouraj, M. M. *Iran. Polym. J.* **2014**, *23*, 257.
16. Zare, E. N.; Lakouraj, M. M.; Mohseni, M. *Synth. Met.* **2014**, *187*, 9.
17. Zare, E. N.; Moghadam, P. N.; Azariyan, E.; Sharifian, I. *Iran. Polym. J.* **2011**, *20*, 319.
18. Wileman, T.; Foster, R. L.; Elliot, P. N. C. *J. Pharm. Pharmacol.* **1986**, *38*, 264.
19. Bahreini, E.; Aghaiypour, K.; Abbasalipourkabir, R.; Mokarram, A.; Goodarzi, M. T.; Saidijam, M. *Nanoscale Res. Lett.* **2014**, *9*, 340.
20. Verma, N.; Kataria, M.; Kumar, K.; Saini, J. *Ann. Biol. Res.* **2013**, *4*, 265.
21. Gasper, M. M.; Blanco, D.; Cruz, M. E.; Alonso, M. J. J. *Control. Release* **1998**, *52*, 53.
22. Vina, I.; Karsakevich, A.; Bekers, M. *J. Mol. Catal. B Enzym.* **2001**, *11*, 551.
23. Kruger, N. *J. Basic Protein Peptide Protocols* **1994**, *32*, 9.
24. Ali, S. M.; Unnikrishnan, G.; Joseph, M. A. *J. Appl. Polym. Sci.* **2013**, *128*, 1409.
25. Grande, C. J.; Torres, F. G.; Gomez, C. M.; Troncoso, O. P.; Canet-Ferrer, J.; Martinez-Pastor, J. *Mater. Sci. Eng. C.* **2009**, *29*, 1098.
26. Kisku, S. K.; Swain, S. K. *Polym. Compos.* **2012**, *33*, 79.
27. Gilliam, M.; Farhat, S.; Zand, A.; Stubbs, B.; Magyar, M.; Garner, G. *Plasma Process. Polym.* **2014**, *11*, 1037.
28. Li, M. C.; Ge, X.; Cho, U. R. *Macromol. Res.* **2013**, *21*, 793.
29. Thomas, P.; Ernest Ravindran, R. S.; Varma, K. B. R. *J. Therm. Anal. Calorim.* **2014**, *115*, 1311.
30. Ghosh, S.; Chaganti, S. R.; Prakashamb, R. S. *J. Mol. Catal. B Enzym.* **2012**, *74*, 132.
31. Youssef, M. M.; Al-Omair, M. A. *Asian J. Biochem.* **2008**, *3*, 337.
32. Ashrafi, H.; Aminic, M.; Mohammadi-Samani, S.; Ghasemi, Y.; Azadi, A.; Tabandeh, M. R.; Kamali-Sarvestani, E.; Daneshamouz, S. *Int. J. Biol. Macromol.* **2013**, *62*, 180.
33. Tavares, A. P. M.; Silva, C. G.; Drazic, G.; Silva, A. M. T.; Loureiro, J. M.; Faria, J. L. *J. Colloid Interface Sci.* **2015**, *454*, 52.
34. Zhang, Y. Q.; Wang, Y. J.; Wang, H. Y.; Zhu, L.; Zhou, Z. Z. *Soft Matter* **2011**, *7*, 9728.
35. Hu, J.; Li, S.; Liu, B. *Biotechnol. J.* **2006**, *1*, 75.